

Cite this: *RSC Adv.*, 2018, 8, 40794Received 17th October 2018  
Accepted 28th November 2018

DOI: 10.1039/c8ra08615j

rsc.li/rsc-advances

# Metallo-supramolecular polymers derived from benzothiadiazole-based platinum acetylide complexes for fluorescent security application†

Ming Yuan,<sup>ac</sup> Feng Wang<sup>id</sup><sup>a</sup> and Yu-Kui Tian<sup>id</sup><sup>\*b</sup>

Metallo-supramolecular polymers with the incorporation of benzothiadiazole-substituted organoplatinum moiety have been successfully constructed. The designed monomer displays intense fluorescence signals, which are severely quenched upon the supramolecular polymerization process. On–off switching of fluorescence can be further exploited for data security materials in response to the chemical stimuli. Accordingly, the resulting supramolecular polymers can be regarded as a novel and efficient candidate toward information processing applications.

Metallo-supramolecular polymers (MSPs), which represent polymeric assemblies constructed by reversible metal–ligand coordination, are considered as an important class of organic/inorganic hybrid supramolecular materials. Owing to the incorporation of metallic complexes in the polymer chain, these macromolecular metal-containing systems not only possess the properties of traditional organic polymers (viscosity, processability, *etc.*), but also exhibit redox, optical, electrochromic, catalytic and magnetic properties.<sup>1–5</sup> In addition, due to the incorporation of reversible and weak recognition moieties on the supramolecular polymeric backbones, MSPs show unique stimuli-responsive characters, which is essential to develop environment-adaptable materials.<sup>6–9</sup>

The structure of MSPs and their physical properties can be elaborately regulated by the coordination ligand motifs.<sup>10,11</sup> Terpyridines and their structural analogs are the most popular chelating end-groups to form MSPs, ascribed to their capability to complex with a variety of transition metals.<sup>10,12–16</sup> Furthermore, the linkage on the polytopic ligand is also of crucial importance, since it dictates the structure arrangement and physicochemical properties of the targeted MSPs assemblies.<sup>10</sup> Up to now, a variety of  $\pi$ -conjugated organic chromophores have been incorporated into the backbone of MSPs.<sup>17–22</sup> In stark contrast, the employment of  $\pi$ -conjugated organometallic units as the linkages has been far-less exploited.<sup>23</sup>

In this work, we sought to attain this objective, and construct a new type of MSPs with the involvement of platinum acetylide

linkage. The monomeric structure is showed in Scheme 1: terpyridine moieties were incorporated on both sides of the monomer, in which the rigid benzothiadiazole-functionalized dinuclear platinum(II) acetylide moiety serves as the linkage unit. Herein, the platinum(II) acetylide derivatives were chosen as the linkages based on the following two considerations. First, platinum(II) acetylide unit features the intriguing photo-physical properties such as larger Stokes shifts and higher photoluminescence quantum yields, which are primarily arised from the overlapping of d-orbitals of the transition metal with p-orbitals of the alkyne ligands.<sup>24–26</sup> As a result, it endows the resulting supramolecular polymers with the fascinating optical and electrochromic properties.<sup>27–31</sup> Second, the rigid linkage incorporated in the monomer structure restrains the tendency for cyclization. The reduced critical polymerization concentration (CPC) value promotes the linear supramolecular polymerization process.<sup>32–35</sup> In the meantime, due to the dynamic properties of metal–ligand interactions, the resulting supramolecular polymer was anticipated to possess the stimuli-responsive properties, which display the potential applications as the smart materials.<sup>36–39</sup>



Scheme 1 Schematic representation for the formation of metallo-supramolecular polymer 1.

<sup>a</sup>CAS Key Laboratory of Soft Matter Chemistry, Department of Polymer Science and Engineering, University of Science and Technology of China, Hefei 230026, P. R. China

<sup>b</sup>Department of Chemistry, Tianjin University, Tianjin 300354, P. R. China. E-mail: yukui.tian@tju.edu.cn; Tel: +86 22 27403475

<sup>c</sup>Clinic Medical College of Anhui Medical University, Hefei 230012, P. R. China

† Electronic supplementary information (ESI) available. See DOI: 10.1039/c8ra08615j



The synthetic route for monomer is quite straightforward. As shown in Scheme S1,<sup>†</sup> Sonogashira coupling reaction between terpyridine and benzothiadiazole-functionalized dinuclear platinum(II) acetylide moieties was employed as the key step to construct the designed monomer. All of the synthetic compounds were fully characterized with NMR and ESI-MS spectra (Fig. S1–S4, ESI<sup>†</sup>). The introduction of dinuclear platinum(II) acetylide unit is expected to achieve low critical polymerization concentration (CPC) value for the supramolecular polymerization process. As a consequence, it facilitates to fabricate fully rigid supramolecular polymers with intriguing optical and electrochromic properties.

Non-covalent complexation between the terpyridine-contained monomer and metal ion  $\text{Zn}^{2+}$  was first investigated *via* the spectroscopic measurements. For the monomer itself, it exhibits two absorption bands with the maximum wavelength located at 358 nm and 477 nm, respectively (Fig. 1a). The high-energy absorption at 358 nm is mainly derived from the  $\pi$ - $\pi^*$  intraligand transitions. For the low-energy absorptions at 477 nm, it could be ascribed to the interplay between the  $\pi$ -conjugated benzothiadiazole acetylene ligand and the transition metal  $\text{Pt}^{2+}$ .<sup>28</sup> With the gradual addition of  $\text{Zn}^{2+}$  to the monomer in  $\text{CHCl}_3/\text{CH}_3\text{OH}$  (2 : 1, v/v), an obvious decrease absorbance at 370 nm was observed (Fig. 1a), indicating the transformation from free terpyridine species to the metal-terpyridine complex.<sup>38</sup> Upon excitation of monomer at 420 nm, the relative quantum yield is determined to be 3.5%, while the emission lifetime is 1.3 ns (Fig. S7<sup>†</sup>). As shown in Fig. 1b, with the stepwise addition of the  $\text{Zn}^{2+}$ , the fluorescence of monomer gradually decreases, and reaches the minimum at 602 nm when the ratio of monomer/ $\text{Zn}^{2+}$  achieves to 1.0. Also, the 1 : 1 complexation was validated by the ITC experiment (Fig. S5<sup>†</sup>).

As widely documented,  $\text{Zn}^{2+}$  could complex with terpyridine to form two kinds of metallic complex species,  $\text{Zn}(\text{tpy})_2^{2+}$  and  $\text{Zn}(\text{tpy})^{2+}$ .<sup>22</sup> However, UV/Vis and fluorescence measurements could not distinctly distinguish such types of complex. In this regard,  $^1\text{H}$  NMR titration measurements were employed to get further insights into the exchange kinetics of  $\text{Zn}^{2+}$ -terpyridine complexes. As shown in Fig. 2, when the feed-ratio of  $\text{Zn}^{2+}$ /monomer is below 1.0 (Fig. 2a–d), the terpyridine proton  $\text{H}_1$  exhibits the remarkable upfield shift from 8.74 to 7.80 ppm due to the shielding effect, while both  $\text{H}_3$  and  $\text{H}_5$  exhibit obviously downfield shifts ( $\text{H}_3$ : from 7.92 to 8.17 ppm;  $\text{H}_5$ : from 8.60 to

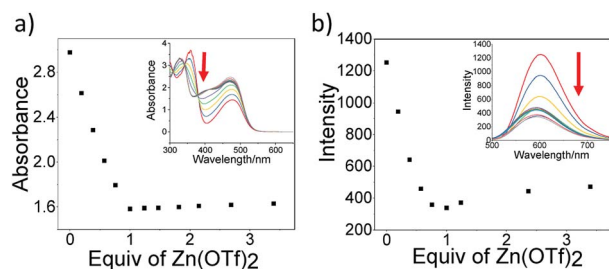


Fig. 1 The intensity of changes (a) absorbance at  $\lambda = 370$  nm and (b) emission intensity at  $\lambda = 602$  nm upon addition of  $\text{Zn}(\text{OTf})_2$ . Insets: arrow shows (a) UV/Vis absorption and (b) emission spectral changes of monomer ( $5.0 \times 10^{-5}$  M) upon addition of  $\text{Zn}(\text{OTf})_2$ .

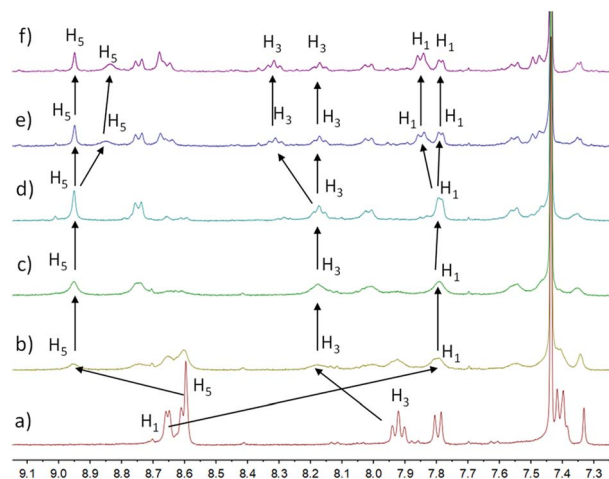


Fig. 2 Partial  $^1\text{H}$  NMR spectra (300 MHz,  $\text{CDCl}_3$ ;  $\text{CD}_3\text{OD}$  (2/1, v/v)): (a) monomer, (b–f) gradual titration of  $\text{Zn}^{2+}$  into monomer.

8.95 ppm). Upon adding 1.0 equivalent  $\text{Zn}^{2+}$ , the original uncomplexed terpyridine signals totally disappeared, suggesting the formation of dimeric  $\text{Zn}(\text{tpy})_2^{2+}$ . However, once  $\text{Zn}^{2+}$ /monomer ratio is further increased, the newly signals evolved and gradually strengthen, suggesting the formation of  $\text{Zn}(\text{tpy})^{2+}$ .<sup>38</sup>

After confirming the non-covalent complexation behavior between  $\text{Zn}^{2+}$  and monomer in relatively low concentration as the monomeric state, the supramolecular polymerization process was further studied *via* concentration-dependent  $^1\text{H}$  NMR measurement. According to Fig. S8,<sup>†</sup> for the 1 : 1 mixture of monomer and  $\text{Zn}(\text{OTf})_2$  at 2.0 mM, the aromatic protons on terpyridine moiety show one set of well-defined sharp signals, implying the dominance of oligomers (Fig. S8a<sup>†</sup>). In sharp contrast, the broadening of all signals at high concentration of monomer suggests the formation of supramolecular polymer (Fig. S8e<sup>†</sup>). Such conclusion could be also validated by two-dimensional diffusion order spectrum experiment (DOSY), which is a convenient and efficient technique to monitor the size variation of the dynamic aggregations. When the monomer concentration increased from 0.5 to 30.0 mM, the measured diffusion coefficients of metallo-supramolecular polymer **1** decreased remarkably from  $2.81 \times 10^{-11}$  to  $8.91 \times 10^{-12}$   $\text{m}^2 \text{s}^{-1}$  (Fig. S9<sup>†</sup>), implying the formation of large-sized supramolecular polymeric assemblies at high concentration.

Next, capillary viscosity measurements were performed to study the macroscopic properties of the resulting supramolecular assemblies. All of the viscosity studies were performed in DMSO containing 0.05 M tetrabutylammonium hexafluorophosphate to exclude the polyelectrolyte effect.<sup>39</sup> As shown in Fig. 3a, the monomer shows the comparably shallow curve for the specific viscosities. In sharp contrast, the specific viscosity of 1 : 1 mixture of  $\text{Zn}^{2+}$  and monomer changes exponentially as a function of monomer concentration, revealing the formation of high-molecular-weight supramolecular polymer.

The double logarithmic plots of *versus* specific viscosity concentration were further obtained for **1** (Fig. 3b), which displays a clear slope change. In the low concentration range,





Fig. 3 (a) Specific viscosities of metallo-supramolecular polymer 1 (red) and the corresponding monomer (blue), (b) double logarithmic plots of specific viscosity of metallo-supramolecular polymer 1 versus monomer concentration.

the slope value was determined to be 1.03, which indicates the presence of oligomers with the constant size. Remarkably, a sharp rise in the viscosity was observed when the concentration exceeds the critical polymerization concentration value (around 4.0 mM), and the slope value was estimated up to 1.40. Such phenomenon is in highly consistent with the aforementioned DOSY and  $^1\text{H}$  NMR results, suggesting the formation of large supramolecular polymeric assemblies at high concentration.

Stimuli-responsive properties of the resulting supramolecular polymer were further exploited, by manipulating the dynamic property of  $\text{Zn}^{2+}$ -terpyridine recognition motif. It is well known that 1,4,7,10-tetraazacyclododecane (cyclen) exhibits higher affinity toward  $\text{Zn}^{2+}$  than terpyridine unit. With the addition of cyclen, the decrease of  $\text{Zn}^{2+}$ /tpy absorption bands ( $\lambda = 477$  nm), together with the increase of fluorescence intensity ( $\lambda = 602$  nm), suggest that cyclen competitively complexes with terpyridine to destroy the  $\text{Zn}^{2+}$ /terpyridine interactions (Fig. 4a, and S10 $^\dagger$ ). Such process could also be validated by capillary viscosity experiments, which is shown in Fig. 4b. With the stepwise addition of cyclen, the specific viscosity of the metallo-supramolecular polymer decreases and gradually levels off, suggesting the disassembly of metallo-supramolecular polymer. However, with the further addition of  $\text{Zn}^{2+}$ , metallo-supramolecular polymer could be recovered. The conclusion could be manifested by the reappearance of  $\text{Zn}^{2+}$ /tpy absorption band, the decrease of fluorescence intensity (Fig. S10 $^\dagger$ ), and the restore of the original  $^1\text{H}$  NMR signals (Fig. S11 $^\dagger$ ). Hence, the successive addition of the competitive

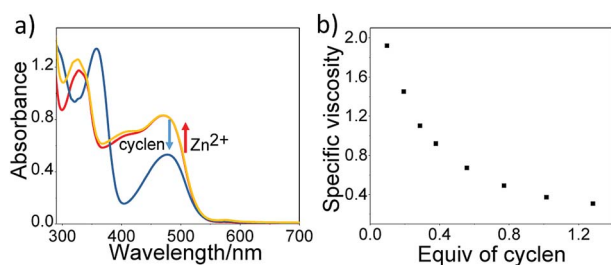


Fig. 4 (a) UV/Vis absorption spectral changes of metallo-supramolecular polymer 1 upon the successive addition of cyclen and  $\text{Zn}(\text{OTf})_2$ . (b) Viscosity changes upon adding cyclen to metallo-supramolecular polymer 1.

ligand cyclen and  $\text{Zn}^{2+}$  provide a possible method to manipulate the reversible assembly/disassembly of the metallo-supramolecular polymer.

As mentioned above, the fluorescence intensity of resulting supramolecular polymers could be regulated by stepwise addition of cyclen and  $\text{Zn}^{2+}$ . By taking advantage of the “on/off” fluorescent switching properties, we sought to explore their potential applications for data security. In detail, the solution of metallo-supramolecular polymer 1 was doped into polylactic acid (PLA) and formed a bright orange film (1.2 cm  $\times$  1.0 cm). The fluorescence intensity of resulting film is relatively lower, owing to the existence of  $\text{Zn}^{2+}$ /terpyridine metal–ligand interactions. The resulting film could be used as a drawing board for the applications in document security, by employing the solution of cyclen as a magic ink (Fig. 5). In detail, when a letter “Z” was written on the surface of the drawing board, there have almost no changes for the film under daylight. However, the patterned security feature of “Z” encrypted with the solution of cyclen could be readily visualized under UV light, which could be ascribed to the disassembly of  $\text{Zn}^{2+}$ -terpyridine complexes. Moreover, the letter “Z” could also be wiped by immersing the film into the  $\text{Zn}^{2+}$  solution and the drawing board could be recovered.

In summary, we have constructed the rigid metallo-supramolecular polymer, by using metal–ligand interactions as the non-covalent connecting bonds. Benzothiadiazole-functionalized dinuclear platinum(II) acetylde moiety was incorporated, rendering fascinating photo-physical properties to the resulting monomer and supramolecular polymeric assemblies.  $^1\text{H}$  NMR, UV/Vis, ITC, DOSY, and viscosity measurements were employed to investigate the supramolecular polymerization process. Additionally, the metallo-supramolecular polymer 1 could be reversibly assembled and disassembled upon adding the competitive ligands. By taking advantage of the fluorescence “on/off” switch process, the resulting supramolecular polymer could be used as fluorescent security materials. Therefore, the current work provides



Fig. 5 Left was irradiated by day light, and right was irradiated by 365 nm. (a) Metallo-supramolecular polymer 1 is doping in the PLA film, (b) cyclen solution is further coated on film, (c) the film is recovered with  $\text{Zn}(\text{OTf})_2$  solution.



a convenient and efficient approach to fabricate supramolecular polymer toward smart information processing materials.<sup>40,41</sup>

## Conflicts of interest

There are no conflicts to declare.

## Acknowledgements

This work was supported by the National Natural Science Foundation of China (21704075, 21871245).

## Notes and references

- G. R. Whittell, M. D. Hager, U. S. Schubert and I. Manners, *Nat. Mater.*, 2011, **10**, 176.
- A. Winter and U. S. Schubert, *Chem. Soc. Rev.*, 2016, **45**, 5311.
- M. Higuchi, *J. Mater. Chem. C*, 2014, **2**, 9331.
- A. Gasnier, G. Royal and P. Terech, *Langmuir*, 2009, **25**, 8751.
- L. Yu, Z. Wang, J. Wu, S. Tu and K. Ding, *Angew. Chem., Int. Ed.*, 2010, **49**, 3627.
- R. J. Wojtecki, M. A. Meador and S. J. Rowan, *Nat. Mater.*, 2011, **10**, 14.
- Y. Han, Y. Tian, Z. Li and F. Wang, *Chem. Soc. Rev.*, 2018, **47**, 5165.
- M. Chiper, R. Hoogenboom and U. S. Schubert, *Macromol. Rapid Commun.*, 2009, **30**, 565.
- J. B. Beck and S. J. Rowan, *J. Am. Chem. Soc.*, 2003, **125**, 13922.
- A. Wild, A. Winter, F. Schluetter and U. S. Schubert, *Chem. Soc. Rev.*, 2011, **40**, 1459.
- A. J. McConnell, C. S. Wood, P. P. Neelakandan and J. R. Nitschke, *Chem. Rev.*, 2015, **115**, 7729.
- M. Burnworth, L. Tang, J. R. Kumpfer, A. J. Duncan, F. L. Beyer, G. L. Fiore, S. J. Rowan and C. Weder, *Nature*, 2011, **472**, 334.
- D. W. R. Balkenende, S. Coulibaly, S. Balog, Y. C. Simon, G. L. Fiore and C. Weder, *J. Am. Chem. Soc.*, 2014, **136**, 10493.
- H. Wang, X. Qian, K. Wang, M. Su, W.-W. Haoyang, X. Jiang, R. Brzozowski, M. Wang, X. Gao, Y. Li, B. Xu, P. Esvara, X.-Q. Hao, W. Gong, J.-L. Hou, J. Cai and X. Li, *Nat. Commun.*, 2018, **9**, 1815.
- L. Gao, Z. Zhang, B. Zheng and F. Huang, *Polym. Chem.*, 2014, **5**, 5734.
- Y. K. Tian, L. Chen, Y. J. Tian, X. Y. Wang and F. Wang, *Polym. Chem.*, 2013, **4**, 453.
- Y. Zhou, H. Y. Zhang, Z. Y. Zhang and Y. Liu, *J. Am. Chem. Soc.*, 2017, **139**, 7168.
- S. Pai, M. Schott, L. Niklaus, U. Posset and D. G. Kurth, *J. Mater. Chem. C*, 2018, **6**, 3310.
- S. Pai, M. Moos, M. H. Schreck, C. Lambert and D. G. Kurth, *Inorg. Chem.*, 2017, **56**, 1418.
- P. Stenclova, K. Sichova, I. Sloufova, J. Zednik, J. Vohlidal and J. Svoboda, *Dalton Trans.*, 2016, **45**, 1208.
- T. Vitvarova, J. Svoboda, M. Hissler and J. Vohlidal, *Organometallics*, 2017, **36**, 777.
- R. Dobrawa, M. Lysetska, P. Ballester, M. Gruene and F. Wuerthner, *Macromolecules*, 2005, **38**, 1315.
- C. Chakraborty, R. K. Pandey, U. Rana, M. Kanao, S. Moriyama and M. Higuchi, *J. Mater. Chem. C*, 2016, **4**, 9428.
- S. Archer and J. A. Weinstein, *Coord. Chem. Rev.*, 2012, **256**, 2530.
- V. Prusakova, C. E. McCusker and F. N. Castellano, *Inorg. Chem.*, 2012, **51**, 8589.
- E. Glimsdal, M. Carlsson, T. Kindahl, M. Lindgren, C. Lopes and B. Eliasson, *J. Phys. Chem. A*, 2010, **114**, 3431.
- H. Masai, J. Terao, S. Makuta, Y. Tachibana, T. Fujihara and Y. Tsuji, *J. Am. Chem. Soc.*, 2014, **136**, 14714.
- X. Wang, Y. F. Han, Y. Y. Liu, G. Zou, Z. Gao and F. Wang, *Angew. Chem., Int. Ed.*, 2017, **56**, 12466.
- E. T. Shi, Z. Gao, M. Yuan, X. Y. Wang and F. Wang, *Polym. Chem.*, 2015, **6**, 5575.
- B. A. D. Neto, P. H. P. R. Carvalho and J. R. Correa, *Acc. Chem. Res.*, 2015, **48**, 1560.
- B. A. D. Neto, J. R. Correa and R. G. Silva, *RSC Adv.*, 2013, **3**, 5291.
- Y. Liu, Y. Yu, J. Gao, Z. Wang and X. Zhang, *Angew. Chem., Int. Ed.*, 2010, **49**, 6576.
- Y. Liu, R. Fang, X. Tan, Z. Wang and X. Zhang, *Chem. Eur. J.*, 2012, **18**, 15650.
- Y. Liu, Z. Huang, X. Tan, Z. Wang and X. Zhang, *Chem. Commun.*, 2013, **49**, 5766.
- R. Joseph, A. Nkrumah, R. J. Clark and E. Masson, *J. Am. Chem. Soc.*, 2014, **136**, 6602.
- H. Hofmeier, R. Hoogenboom, M. E. L. Wouters and U. S. Schubert, *J. Am. Chem. Soc.*, 2005, **127**, 2913.
- G. Groeger, W. Meyer-Zaika, C. Boettcher, F. Groehn, C. Ruthard and C. Schmuck, *J. Am. Chem. Soc.*, 2011, **133**, 8961.
- Y. Ding, P. Wang, Y. K. Tian, Y. J. Tian and F. Wang, *Chem. Commun.*, 2013, **49**, 5951.
- Y. K. Tian and F. Wang, *Macromol. Rapid Commun.*, 2014, **35**, 337.
- Z. Gao, Y. Han and F. Wang, *Nat. Commun.*, 2018, **9**, 3977.
- Z. Gao, Y. Han, Z. Gao and F. Wang, *Acc. Chem. Res.*, 2018, **51**, 2719.

